Applied Catalysis B: Environmental 187 (2016) 408–418

Contents lists available at ScienceDirect

Applied Catalysis B: Environmental

journal homepage: www.elsevier.com/locate/apcatb

A bimetallic catalyst on a dual component support for low temperature total methane oxidation

Ahmed I. Osman[a,b], Jehad K. Abu-Dahrieh[a], Fathima Laffir[c], Teresa Curtin[c], Jillian M. Thompson[a,*], David W. Rooney[a,*]

[a] CenTACat, School of Chemistry and Chemical Engineering, Queen's University, David Keir Building, Stranmillis Road, Belfast, BT9 5AG Northern Ireland, United Kingdom
[b] Chemistry Department, Faculty of Science—Qena, South Valley University, Qena 83523, Egypt
[c] Department of Chemical and Environmental Sciences, Materials and Surface Science Institute, University of Limerick, Limerick, Ireland

ARTICLE INFO

Article history:
Received 30 October 2015
Received in revised form
23 December 2015
Accepted 9 January 2016
Available online 14 January 2016

Keywords:
Palladium
Platinum
Titania
Zeolite
Methane oxidation

ABSTRACT

Palladium, platinum bimetallic catalysts supported on η-Al_2O_3, ZSM-5(23) and ZSM-5(80), with and without the addition of TiO_2, were prepared and used for low temperature total methane oxidation (TMO). The catalysts were tested under reaction temperatures of 200–500 °C with a GHSV of 100,000 mL g^{-1} h^{-1}. It was found that all four components, palladium, platinum, an acidic support and oxygen carrier were needed to achieve a highly active and stable catalyst. The optimum support being 17.5% TiO_2 on ZSM-5(80) where the $T_{10\%}$ was observed at only 200 °C. On addition of platinum, longer time on stream experiments showed no decrease in the catalyst activity over 50 h at 250 °C.

1. Introduction

Methane is an abundant resource which can be found in large quantities in natural gas reserves and can be produced from bioderived sources through, for example, anaerobic digestion [1,2]. However, its high symmetry and resulting stability makes direct conversion to liquid fuels or chemical feed stocks inherently challenging and direct conversion to higher value chemicals to date is uneconomical [3,4] when compared with syngas routes [5–7].

As a fuel, natural gas is very attractive as it generally contains low levels of pollutants such as nitrogen or sulfur and produces low levels of CO_2 per energy produced [8]. However, complete combustion can be difficult to achieve with traces often released in the exhaust gas streams and given its global warming potential this is problematic [9].

Furthermore CO and, depending on the source of the gas, SO_x species from impurities in the feed [10] can be produced. Also at high combustion temperatures NO_x can be formed thereby necessitating the development of catalytic systems to facilitate complete combustion at low temperatures [11–14].

Many metals have been studied as methane combustion catalysts including platinum [11,15], palladium [16–18], and copper [19] with palladium being recognised as the most active [12,20,21]. Carstens et al. [22] reported that the mechanism of reaction occurs through dissociative adsorption of CH_4, preferentially on metallic palladium and subsequent oxidation by PdO species. Their studies on a Pd/ZrO_2 catalyst showed that activity increased, up to a maximum, with an increasing proportion of surface PdO. This activity was enhanced by the presence of small amounts of reduced Pd on the catalyst surface allowing dissociative adsorption. This is in agreement with Burch et al. [20] who showed that the activity increased until an optimum oxide coverage of approximately 3–4 monolayers was obtained. Lin et al. using $^{18}O_2$ species over a pre-oxidised $Pd/TiO_2/Al_2O_3$, catalyst [12] also agreed with this mechanism. Therefore, Pd(0) is required to adsorb methane while PdO species are needed for oxidation. It is known that the PdO/Pd(0) redox cycle can be controlled by addition of an oxygen carrier such as TiO_2 to the support. For example Lin et al. [12] reported a decrease in $T_{10\%}$ of 30 °C on addition of 20 wt% TiO_2 but the best catalyst still showed a $T_{10\%}$ greater than 250 °C at a space velocity of 33,000 mL h^{-1} g^{-1}, one third of that used herein.

* Corresponding authors.
E-mail addresses: jillian.thompson@qub.ac.uk (J.M. Thompson), d.rooney@qub.ac.uk (D.W. Rooney).

http://dx.doi.org/10.1016/j.apcatb.2016.01.017
0926-3373/

Palladium complex species are reported to be more electron deficient on more acidic supports compared to neutral supports [23–25]. This increased electrophilicity alters the Pd(0)/PdO redox cycle and therefore catalyst activity. Stakheev et al. [25] used XPS while Wang et al. [26] used DFT calculations to assess the effect of support acidity on PdO bond strength which was found to increase with the number of protons present on a ZSM-5 surface. M'Ramadj et al. [18] recognised the role of support acidity in methane combustion over Pd/ZSM-5 and reported a $T_{10\%}$ of most catalysts ranging from 220 to 400 °C at a space velocity of 36,000 h^{-1}.

This equilibrium between PdO and Pd(0) is also affected by a number of parameters such as temperature, oxygen partial pressure, metal particle size and interaction with the support [27]. However poor stability of the PdO at temperatures between 650 and 850 °C due to Pd(0) formation and irreversible sintering presents major obstacles. Addition of CeO_2 can inhibit this deactivation and recently Cargnello [28] described the preparation of a Pd@CeO_2 core shell catalyst on functionalised Al_2O_3 which remained stable over 5 runs. However even with such specifically designed materials, analysis by Zhang [29] shows formation of clouds of palladium resulting in an intimately mixed Pd/Ce/SiO_2 mixed species at elevated temperatures.

Comparison of Pd, Pt and their combination has shown that the addition of a second metal limits deactivation [30] and a $T_{10\%}$ as low as 228 °C was observed with a 0.2 wt% Pt and 0.3 wt% Pd bimetallic catalyst supported on TiO_2 at a space velocity of 21,000 h^{-1}. Improved stability of Pd/Pt bimetallic catalysts was also reported by Persson et al. with a $T_{10\%}$ between 450 and 750 °C at a space velocity of 250,000 h^{-1} [14]. This has been attributed to either the Pt preventing the particle growth of the PdO [31], a change in the morphology or metal loss from the monometallic palladium catalyst [32]. Although there is some debate in the literature about increased activity with bimetallic catalysts [14], it is generally accepted that the bimetallic is more stable.

It should be noted that under realistic operating conditions water, sulfur, nitrogen and phosphorous containing compounds also affect performance. The effect of such additives is dependent on the combination present and also the support [33] Addition of 15% water to a hierarchical Pd@CeO_2/Si-Al_2O_3 catalyst resulted in deactivation [34], however no deactivation was observed over a similar Pd@ZrO_2 catalyst with 10% water in the feed [35]. Gremminger et al. [36] carried out an extensive study on catalyst poisoning of PdPt/Al_2O_3, identifying SO_2 as the most detrimental.

The above discussion leads to the conclusion that a bimetallic catalyst should be used together with a support containing both oxygen transport and acidic components. Hence at least four components would be required for low temperature operation. Herein we demonstrate that such a four component catalyst, based on a bimetallic catalyst (Pd/Pt) for stability, TiO_2 for oxygen mobility and an acidic support (η -Al_2O_3 or H-ZSM-5) for the reoxidation of Pd(0), is superior to simpler catalysts. This four component catalyst has been optimised within the parameters used and facilitates methane combustion with a $T_{10\%}$ of 200 °C at realistic space velocities of 100,000 mL g^{-1} h^{-1}.

2. Experimental

2.1. Materials

The chemicals used in the present study were all analytical grade, from Sigma-Aldrich, UK or Alfa Aesar and were used without further purification. Aluminium nitrate nonahydrate (≥98%), ammonia solution (35%), palladium (II) nitrate dihydrate ($Pd(NO_3)_2{\cdot}2H_2O$, ~40% Pd basis), potassium tetrachloropalladate (II) (K_2PdCl_4, ≥99.995%), ammonium tetrachloroplatinate (II) ($(NH_4)_2PtCl_4$, 99%), titanium (IV) oxide anatase nanopowder (TiO_2, 99.7%) were all obtained from Sigma-Aldrich. Zeolite H-ZSM-5(80) (SiO_2:Al_2O_3 80:1 mol ratio), zeolite H-ZSM-5(23) (SiO_2:Al_2O_3 23:1 mol ratio) and tetraammineplatinum (II) hydroxide in solution ($Pt(NH_3)_4(OH)_2$, assay 9.09%) were obtained from Alfa Aesar. All gases Ar, CH_4, O_2/Ar and Ne were obtained at 100% purity from BOC gases, UK.

2.2. Catalyst preparation

2.2.1. The supports

The preparation of the alumina support has been described in a previous work [37]. For the aluminium nitrate precursor, after the precipitation by ammonia solution, the resulting precipitate was calcined at 550 °C and designated as AN550. H-ZSM-5(80) and H-ZSM-5(23) were used as received.

2.2.2. Preparation of bimetallic Pd/Pt on η-Al_2O_3 or on H-ZSM-5 supports with the addition of TiO_2

Bimetallic catalysts were prepared by a wet impregnation method with the aid of sonication. Pure supports AN550, H-ZSM-5(80) or H-ZSM-5(23) were placed in a vial and the mass of metal precursor solution or slurry, required to give a 5 wt% palladium and 2 wt% platinum loading was added followed by TiO_2 to give 25 wt% in deionised water (5 mL). The mixture was sonicated at 80 °C (Crest ultrasonic bath model 200HT), under a 45 kHz frequency for 3 h. All mixtures were dried at 120 °C overnight in an oven before being calcined in air at 500 °C for 4 h with a heating ramp of 2 °C min^{-1}.

Six catalysts with the compositions given below, in wt%, were prepared to determine the effect of the precursor and support used. All catalysts contained 25%TiO_2.

Catalyst 1: 5% Pd (NO_3) + 2% Pt (Cl) + 68% AN550
Catalyst 2: 5% Pd (Cl) + 2% Pt (NH_3) + 68% AN550
Catalyst 3: 5% Pd (Cl) + 2% Pt (Cl) + 68% AN550
Catalyst 4: 5% Pd (Cl) + 2% Pt (Cl) + 68% H-ZSM-5(80)
Catalyst 5: 5% Pd (NO_3) + 2% Pt (NH_3) + 68% H-ZSM-5(80)
Catalyst 6: 5% Pd (NO_3) + 2% Pt (NH_3) + 68% H-ZSM-5(23)

The chlorinated catalysts (1 to 4) were further washed with deionised water until no halide was detected using $AgNO_3$. The washed catalysts were calcined in air at 250 °C for 3 h with a heating rate of 2 °C min^{-1}.

2.2.3. Different TiO_2 loadings on PdPt/H-ZSM-5(80)

The catalysts used to study the effect of TiO_2 loading were based on the metal (Pd and Pt) precursors and loadings used in Cat 5. The metal loading was 7 wt% with the overall support being 93 wt% of the catalyst. A range of titania loadings of (0, 5, 10, 17.5, 25, 35, 46.5, 68 and 83 wt% TiO_2) on H-ZSM-5(80) were prepared by altering the mass of H-ZSM-5(80) and TiO_2 used. After drying, the catalysts were calcined in air at 500 °C for 4 h with a heating ramp of 2 °C min^{-1}. Catalysts are denoted as: 0%TiO_2, 5%TiO_2, 10%TiO_2, 17.5%TiO_2, 25%TiO_2 (Cat 5), 35%TiO_2, 46.5%TiO_2, 68%TiO_2 and 83%TiO_2.

2.2.4. Effect of preparation method, metal dispersion and sonication

The effects of the preparation method on the observed rate of reaction were tested by preparing a 5% Pd (NO_3), 2% Pt (NH_3), 17.5 wt% TiO_2 and 75.5 wt% H-ZSM-5 (80) catalyst in three different ways to that described in Section 2.2.3, Cats 7–9.

For Cat 7, TiO_2 was placed in the vial first, followed by the solutions of the metal precursors and finally the H-ZSM-5. The mixture was sonicated, dried and calcined according to Section 2.2.2. Cats 8 and 9 were prepared as per Cat 7 but with TiO_2 either ground together thoroughly with the bimetallic zeolite catalyst (Cat 8) or added in water and sonicated before drying and calcination (Cat 9).

Cats 10 and 11 contained 7% Pd (NO_3) and 7% Pt (NH_3) respectively with the balance being 17.5%TiO_2 + 75.5% ZSM-5(80). Catalyst 12 was composed of 1 wt% Pd, 0.4 wt% Pt, 18.6 wt% TiO_2 and 80 wt% ZSM-5(80). Catalyst 13 had the same composition as the reference 17.5%TiO_2 but rather than suspending the vial in an ultrasonic bath at 80 °C, it was suspended in a water bath at this temperature. Tests carried out with three different batches of catalyst confirmed the reproducibility.

2.3. Catalyst characterization

The catalysts were characterized by powder X-ray diffraction (XRD) using a PANalytical X'Pert Pro X-ray diffractometer. This diffractometer was equipped with a CuKα X-ray source with a wavelength of 1.5405 Å. The diffractograms were collected up to 80°. The X-ray tube was set at 40 kV and 40 mA.

Brunauer-Emmett-Teller (BET) analysis was performed using a Micromeritics ASAP 2010 system. The BET surface areas and pore volumes were measured by N_2 adsorption and the desorption isotherm at −196 °C at relative pressures between 0.5 and 0.9. The chloride content was measured using Oxygen Flask analysis.

The Scanning Electron Microscope used was a FEI Quanta 250 FEG MKII with a high resolution environmental microscope (ESEM), XT microscope control software and EDX detector. The EDX had a 10 mm^2 SDD Detector-x-act (Oxford Instruments) utilizing Aztec® EDS analysis software. Both systems used the same chamber. Three different samples of each catalyst were measured at ten different points and these measurements averaged.

Temperature-programmed reduction (TPR) was carried out using a Micromeritics Autochem 2910 with H_2 uptake monitored by a TCD. The catalyst sample (0.1 g) was placed in a quartz tube and cooled under Ar until −20 °C. 5% H_2/Ar with a flow rate of 30 mL min^{-1} was passed over the catalyst until a stable baseline was obtained after which the sample was heated at 10 °C min^{-1} up to 700 °C.

XPS was performed in a Kratos AXIS 165 spectrometer using monochromatic Al Kα radiation of energy 1486.6 eV. High resolution spectra of Pd 3d were taken at a fixed pass energy of 20 eV, 0.05 eV step size and 100 ms dwell time per step. Surface charge was efficiently neutralised by flooding the sample surface with low energy electrons. Core level binding energies were corrected using the C 1s peak at 284.8 eV as charge reference. For construction and fitting of synthetic peaks of high resolution spectra, a mixed Gaussian-Lorenzian function with a Shirley type background subtraction were used.

2.4. Catalyst activity

The activity testing was carried out in an isothermal fixed-bed reactor made of stainless steel (6 mm OD) at atmospheric pressure. The catalyst bed consisted of 50 mg of catalyst, pelletized and sieved to between 250 and 425 μm, placed between two plugs of quartz wool. Aera mass flow controllers were used to control the flow of Ar, CH_4, O_2/Ar and Ne. Prior to the catalytic tests, each catalyst was oxidized under a flow of 5% O_2/Ar at a flow rate of 40 mL min^{-1} at 500 °C for 2 h with a heating rate 5 °C min^{-1}. The reaction gas mixture, which consisted of 0.5% CH_4, 10% O_2, 5% Ne and 84.5% Ar, was then fed to the fixed bed reactor with the total flow maintained at 83.3 mL min^{-1}, giving a GHSV of 100,000 mL g^{-1} h^{-1}. The products were analyzed by on-line gas chromatography using a Perkin Elmer 500 GC equipped with a Haysep column and TCD and FID detectors. The internal standard was 5% Ne in the feed. Reaction temperature was monitored throughout by a thermocouple placed in the centre of the catalyst bed. Under the conditions used no exotherm was observed.

Table 1
Composition of catalysts as determined from EDX/SEM analysis.

	Pd	Pt	O	Ti	Si	Al
0%TiO_2	2.7	1.5	60	–	35	0.8
5%TiO_2	3.4	2.1	60.2	3	30.6	0.7
17.5%TiO_2	5.1	1.5	57.9	8.5	26.5	0.6
46.5%TiO_2	4.3	2.1	57.8	20.3	15.5	–
Cat 8	3.6	1.4	56.0	8.6	29.7	0.7
Cat 10	5.3	–	58.3	8.5	27.2	0.7
Cat 11	–	7.2	54.2	9	29	0.7

3. Results and discussion

3.1. Catalyst characterization

The surface areas and pore volumes, as measured by BET are shown in Table S1 and reflect the surface areas of the supports from which they were prepared. The lower surface area alumina 223 m^2 g^{-1} [37] and higher surface area H-ZSM-5 zeolite 425 m^2 g^{-1} resulted in catalysts with surface areas of 129 and 223 m^2 g^{-1}, respectively. As expected, as the amount of TiO_2 deposited onto the surface increased the surface area of the catalyst decreased with a corresponding increase in pore volume from 0.08 cm^3 g^{-1} to 0.26 cm^3 g^{-1}.

XRD analysis of the AN550 and TiO_2 supports are shown in Fig. S1a along with those for Catalysts 1–3 which were all prepared from the AN550 support. The AN550 showed diffraction lines that correspond to η-Al_2O_3 (JCDD 04-0875) [37], and the TiO_2 diffraction lines corresponding the anatase phase (JCPDS 21-1272). On deposition of the palladium and platinum metals, a band at 2θ = 33.8° from PdO [14] and another very small band at 2θ = 39.7° corresponding to the combined bimetallic palladium platinum (PdPt) phase [14,38] is observed in Cat 1 and Cat 2.

The XRD for H-ZSM-5(80) and associated catalysts are shown in Fig. S1b along with the TiO_2 for reference. Again on deposition of palladium and platinum, the peak from PdO and the very small peak from PdPt can be observed. Fig. 1 shows the XRD patterns for the catalysts based on Cat 5, with varying loadings of TiO_2. As expected, the diffraction lines that correspond to H-ZSM-5(80) decrease in intensity on increasing TiO_2 loading with a consequent increase in intensity of peaks from TiO_2. Again the peak from PdO is clearly observed for all catalysts at decreasing intensity with increasing TiO_2 loading, Fig. S2.

3.1.1. SEM and EDX

SEM images, Fig. S3, show that the surface texture of the catalyst changes with TiO_2 loading. For 0%TiO_2, small crystals are present whereas for 83%TiO_2 these are no longer visible being replaced by larger, smoother particles.

Table 1 shows an apparent composition of the catalysts as determined by EDX analysis. The platinum loading measured varied only slightly throughout the samples, however, the amount of palladium metal changed between samples. The Ti content increased with increasing TiO_2 deposition as expected.

3.1.2. H_2-TPR

The H_2-TPR spectra for Cat 1, Cat 5, H-ZSM-5(80), AN550 and TiO_2 are given in Fig. S4 and shows that the nature of the Pd on each support is different. There is no reduction peak for the AN550 and ZSM-5(80) supports in the temperature range from −20 °C to 700 °C [39] whereas the TiO_2 support showed a broad reduction peak in the temperature range 330–550 °C, which can be attributed to the reduction of Ti^{4+} to Ti^{3+} [40].

Cat 1 showed a number of reduction peaks with those at 300 and 517 °C attributed to the reduction of TiO_2 in different environments and those at lower temperatures from the reduction of the PdO. Cat

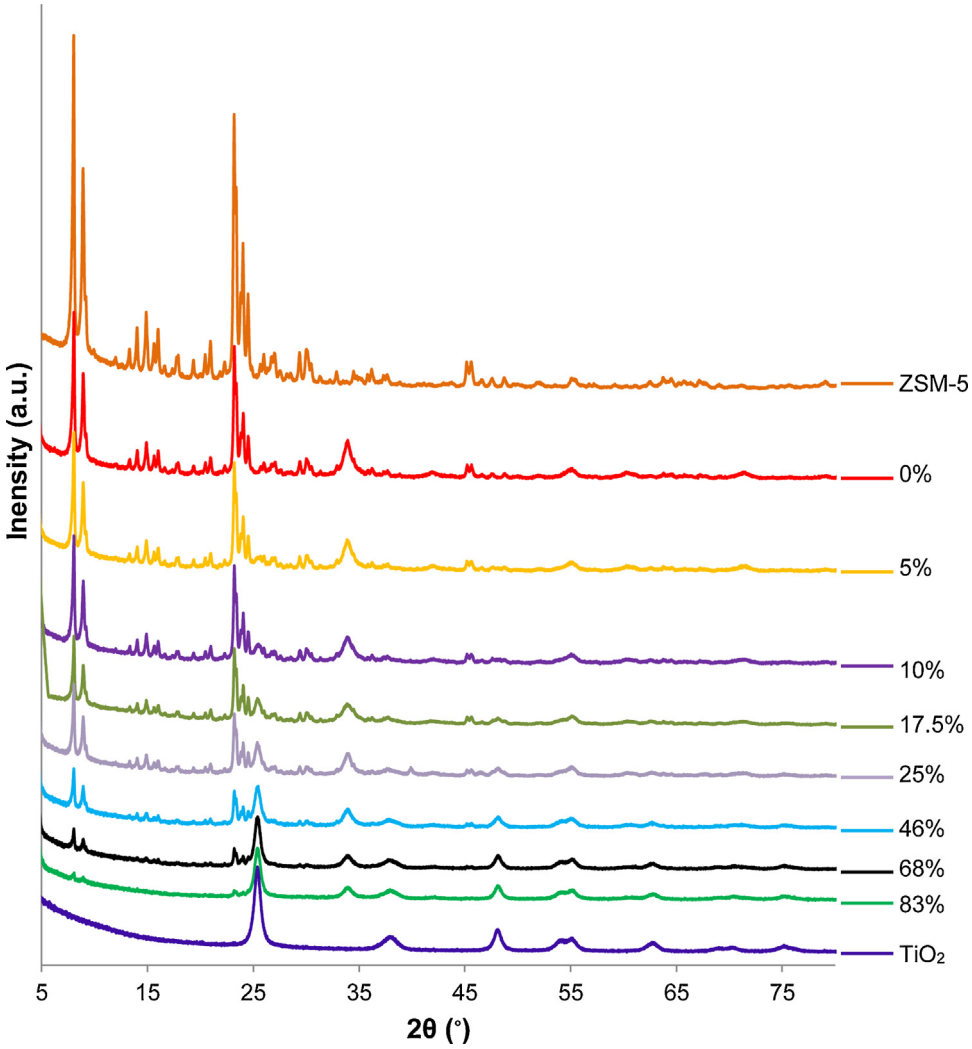

Fig. 1. XRD patterns of Cat 5, (5 wt% Pd, 2 wt% Pt on H-ZSM-5(80)) with different TiO_2 (wt%) loadings.

5 also showed a reduction peak around 300 °C from the reduction of TiO_2 but in addition to the positive peaks at 18 and 70 °C, from the reduction of PdO, there is a negative peak at 59 °C from the decomposition of the Pd β-hydride [12].

3.2. Catalyst activity

The only products observed by GC analysis of the outlet stream of the reactor were CO_2 and H_2O confirming that only the TMO reaction was occurring. In all cases, a C balance greater than 99% was obtained.

Comparison of the activity of catalysts prepared from chlorinated salts with those formed from non chlorinated salts showed a greatly decreased activity. Fig. S5 and Table S2 show that irrespective of the support, catalysts prepared from Pd precursors containing chloride showed no activity below 300 °C. However activity could be greatly improved by simply washing these catalysts (Fig. S6). These results are in agreement with work by the groups of Lin, Simone and Roth [12,41,42] who showed that the presence of residual chloride inhibited the reaction due to the adsorption of chloride on the metal surface. All subsequent catalysts were therefore prepared from the non-chlorinated precursors used for Cat 5.

As previously discussed there is strong evidence that the activity of TMO catalysts will be improved by an optimised ratio of between PdO and Pd(0) [12,22]. It is also known that the presence of Bronsted acidity on the support will make the Pd species electron deficient potentially enhancing the reoxidation of any Pd(0) [26]. To test the connection between these parameters, catalysts prepared from the same metal precursors and TiO_2 loading were prepared on a η-alumina support with a mixed Lewis and Bronsted acidity (Cat 3) and a zeolite support with stronger Bronsted acidity (Cat 4) [37]. Comparisons given in Table S2 shows that the catalyst prepared on the zeolite containing the stronger acid sites is significantly more active with $T_{50\%}$ values of 344 °C and 256 °C for the alumina and H-ZSM-5(80) catalysts respectively.

Cat 5 was also used as a benchmark to test the effect of varying TiO_2 loading. As described earlier, as the TiO_2 loading increased from 0% to 83%, the BET surface area decreased, Table S1 and the anatase TiO_2 peak in the XRD increased, with the zeolite peaks all but disappearing above 46.5 wt% TiO_2, Fig. 1.

The activity of the TiO_2 doped catalysts are shown in Fig. 2 and the $T_{10\%}$, $T_{50\%}$ and $T_{90\%}$ values given in Table 2.

The increase and subsequent decrease in activity with increasing TiO_2 loading is clearly not dependent on the surface area of the catalysts, Table S1; or the amount of PdO species present, Fig. S2. However, the effect of oxygen supply on the conversion can be seen from the curves shown in Fig. 2. Comparison of the $T_{50\%}$ and $T_{90\%}$ values shows that the TiO_2 loading has a greater influence on the reaction at higher conversions. The difference in the $T_{50\%}$

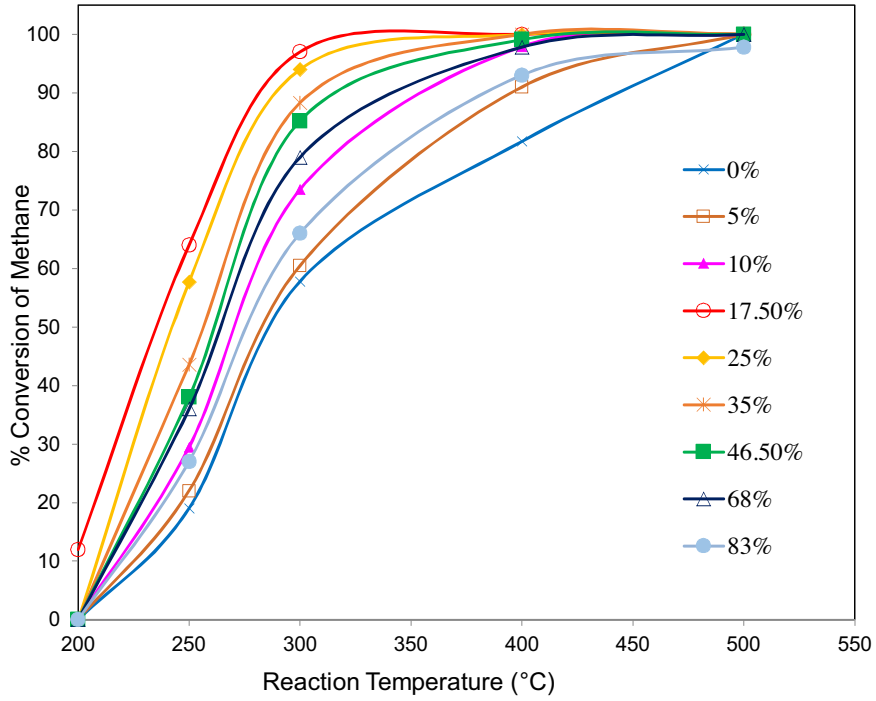

Fig. 2. Catalytic activity profiles for methane oxidation over Cat 5, 5 wt% Pd, 2 wt% Pt on ZSM-5(80) with different TiO_2 loadings.

values for all the catalysts tested is only 51 °C but 161 °C at $T_{90\%}$, indicating that a different limitation is controlling the reaction at different TiO_2 loadings. When there is no TiO_2 present, (0%TiO_2, Fig. 2) the change in the gradient of the curve at high conversion is attributed to a fast rate of reaction which becomes limited by oxygen transport [43]. The addition of 5 wt% TiO_2 causes little change to the start of the curve but does result in a considerable difference at high temperatures as demonstrated by only a 3 °C decrease in the $T_{50\%}$ value but a 47 °C decrease in the $T_{90\%}$ value. It is proposed that here, the presence of even a small amount of TiO_2 improves the oxygen supply at high conversions. As the loading of TiO_2 is increased the change in the gradient of the curve is less noticeable until at 17.5 wt% and 25 wt% TiO_2 the curve is linear until almost complete conversion showing no oxygen limitation. However, further addition of TiO_2, above 25 wt% resulted in a decrease in the activity of the catalyst. A change in slope at higher temperatures was again observed, with the 83%TiO_2 catalyst showing similar behaviour to the 10%TiO_2 catalyst. At these high loadings of TiO_2, there is a ready transport of oxygen however the decreasing surface area along with the decreased acidity leads to lower metal dispersion and reduced electrophilicity of Pd(0) both of which could contribute to the decreased activity.

Table 2
The temperature required to reach 10% ($T_{10\%}$), 50% ($T_{50\%}$) and 90% ($T_{90\%}$) conversion for the combustion of methane using catalysts prepared on the ZSM-5(80) support, with 5 wt% Pd, 2 wt% Pt and X wt% TiO_2.

Percentage by weight of TiO_2 on the support (X)	$T_{10\%}$ (°C)	$T_{50\%}$ (°C)	$T_{90\%}$ (°C)
0%TiO_2	231	286	443
5%TiO_2	226	283	396
10%TiO_2	218	270	356
17.5%TiO_2	198	235	282
25%TiO_2 (Cat5)	208	240	290
35%TiO_2	212	255	306
46.5%TiO_2	214	262	316
68%TiO_2	215	264	342
83%TiO_2	220	276	384

The conversion of methane at 250 °C is shown in Fig. 3 where the optimum TiO_2 loading of the catalysts tested is 17.5 wt%. This optimum is similar to the findings of Lin et al. [12] who showed that 19 wt% TiO_2 loaded onto an alumina support gave a more active catalyst than either 8.8 wt% or 24 wt% loading.

3.3. Nature of Pd species

As the activity of the catalysts showed a clear dependence on the TiO_2 loading and possible oxygen limitation, the redox behaviour of the palladium species was examined using TPR and XPS analysis. The effect of increasing TiO_2 loadings on the Pd species present is shown in the TPR analysis (Fig. 4).

For all catalysts containing TiO_2, the TiO_2 reduction occurs in the range of 220–420 °C, significantly lower than for the pure TiO_2 due to the influence of the palladium [44]. For 0 wt%, 5 wt% and 10 wt% TiO_2 catalysts, a broad peak from the reduction of PdO to palladium metal is observed between −20 and 100 °C [45,46]. In the absence of TiO_2 this peak is at 8 °C and with increasing TiO_2 loading, this reduction occurs more readily and the peak appears at −2 °C at 10 wt% loading. Similar decreased reduction temperatures have been reported by Lin et al. [12] and by Wang et al. [46] for TiO_2 on alumina supported catalysts. As the TiO_2 loading is increased further, to 17.5 wt%, Fig. 4b, the PdO reduction peak decreases in intensity and another peak, this time negative, at around 38 °C is formed which is attributed to the decomposition of the β-hydride of the palladium metal [47–49]. The decrease in intensity of the PdO reduction peak with increasing TiO_2 loading along with the reduced PdO peak in the XRD, Fig. S2, indicates a decrease in PdO stability on the catalyst surface as the amount of TiO_2 is increased. This implies the palladium species on the catalysts with higher TiO_2 loadings are more readily reducible. The presence of both negative and positive peaks for catalysts with intermediate TiO_2 loadings of 17.5, 25, 35 and 46.5 wt% indicates a facile reduction/oxidation cycle and the potential for the presence of two phases of palladium, PdO and Pd(0) under reaction conditions.

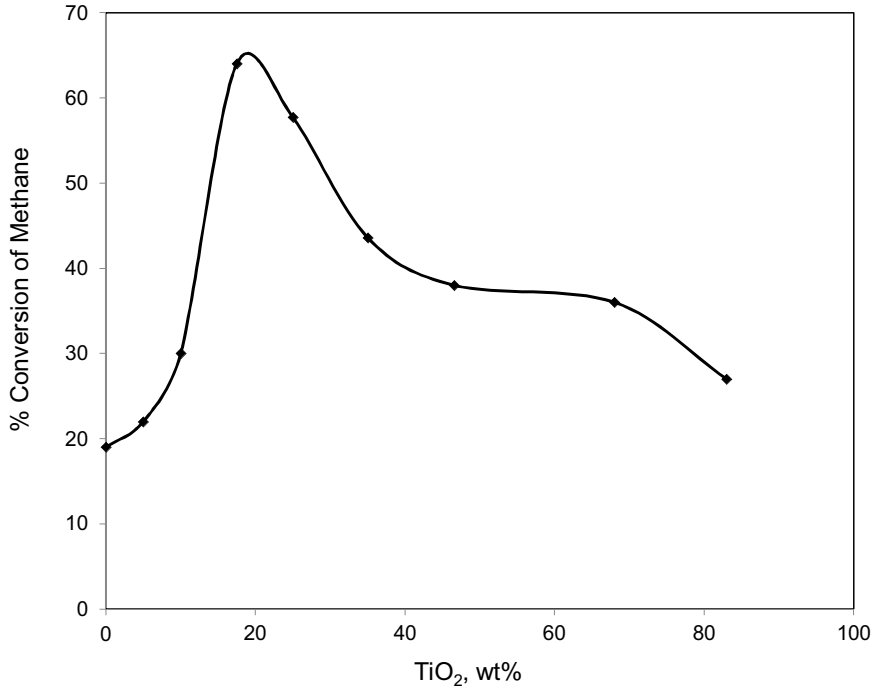

Fig. 3. Summary of the catalytic activity for methane oxidation over Cat 5, 5 wt% Pd, 2 wt% Pt on ZSM-5(80) with different TiO_2 loadings.

As the TiO_2 loading is increased further to greater than 68 wt%, the positive peak disappears corresponding to the decreased PdO content of the catalyst as shown in the XRD, leaving the negative peak from β-hydride decomposition as the only low temperature peak.

As the number of acid sites on the zeolite support can control the redox behaviour of the Pd adsorbed on the surface [25,26]. H-ZSM-5

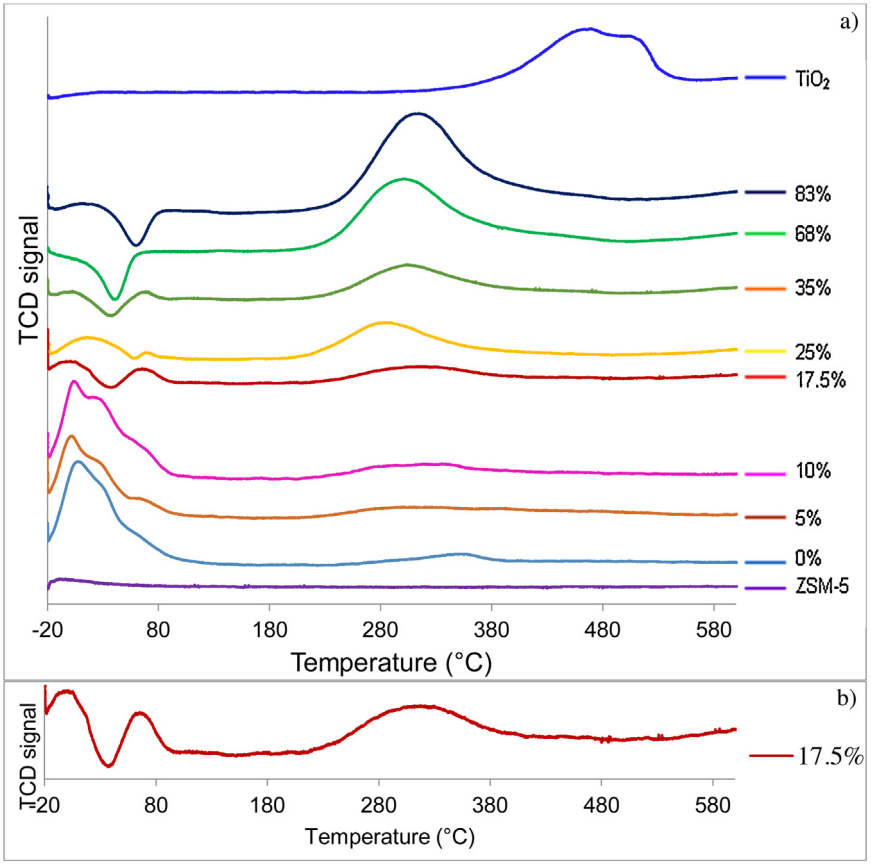

Fig. 4. H_2-TPR profiles of a 5 wt% Pd, 2 wt% Pt, H-ZSM-5(80) with different TiO_2 loadings. TiO_2 and ZSM-5(80) are the titania and zeolite supports. b Expansion of the H_2-TPR profile of catalyst containing 17.5 wt% TiO_2.

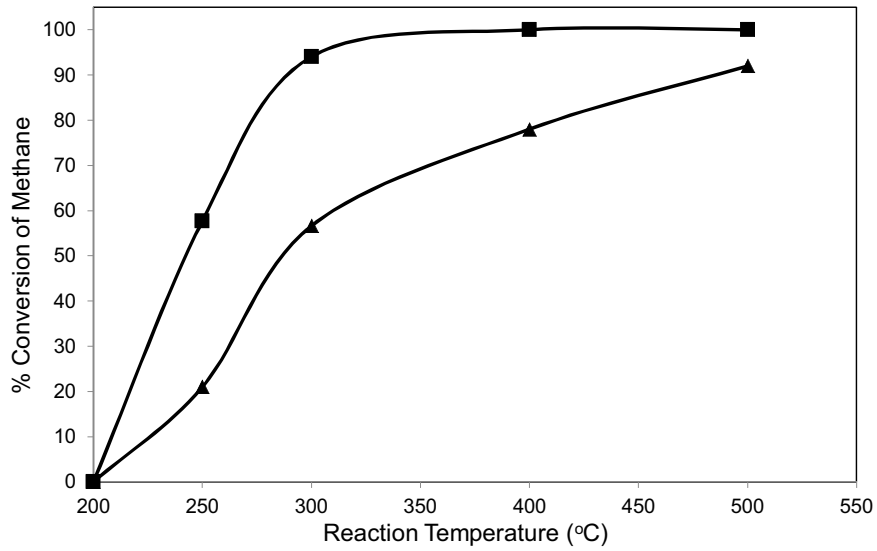

Fig. 5. Catalytic activity profiles for methane oxidation over 5 wt% Pd, 2 wt% Pt on ZSM-5(80) (■) and H-ZSM-5(23) (▲), each with 25 wt% TiO_2.

with a SiO_2:Al_2O_3 ratio of 23 was used (Cat 6) to further investigate the role of electrophilicity on the catalyst activity. Fig. 5 shows that the catalyst prepared on H-ZSM-5(23) is not as active as that on H-ZSM-5(80) with $T_{10\%}$ increasing from 208 °C for H-ZSM-5(80) to 226 °C for H-ZSM-5(23), Table S2.

The XPS analysis in Fig. 6 shows the palladium 3d region of the spectra. There was no indication of the presence of any Pt/Pd alloy and the palladium was predominantly present as PdO with a binding energy of approximately 336.8 eV with a minor contribution from PdO_2 shown by the peak at 338.0 eV [50]. Only a small contribution from metallic Pd was observed, shown by small peaks at around 335.2 eV for all TiO_2 containing catalysts.

The XPS analysis of the selection of catalysts shown in Fig. 6 supports the changing redox character of the catalysts with varying TiO_2 loading and zeolite acidity. As the TiO_2 loading is increased the binding energy of the PdO ($Pd_{5/2}$) species decreased from 337.0 eV for 0%TiO_2 to 336.8 eV for 17.5%TiO_2 and 25.5%TiO_2 and further to 336.6 eV for 83%TiO_2 signifying a less electron deficient palladium species. In addition, a small increase in binding energy from 336.8 eV to 336.9 eV was observed on changing the acidic support from H-ZSM-5(80) to H-ZSM-5(23) which could indicate a slight increase in electron deficiency of the palladium species with increasing number of protons.

The facile redox cycle implied by the TPR and XPS data of the optimised catalysts is in agreement with the literature, with Burch et al. and Carsten et al. reporting the need for both metallic and oxidic palladium to be present [20,22].

It can therefore be concluded from TPR and XPS analysis that the TiO_2 loading and support acidity influences the redox behaviour of the palladium species and as a consequence the activity of the catalyst. With increasing TiO_2 loading the palladium species shows decreased PdO character as evidenced from the decreased intensity of the peak at $2\theta = 33.8^\circ$ in the XRD, the negative peak in the TPR analysis and the change in binding energy in the XPS. The optimised catalyst composition is therefore achieved through a balance of an acid support for increased electrophilicity which promotes rapid oxidation and an oxygen carrier for assisting reduction and oxygen transport. If the TiO_2 loading is less than this optimum the palladium is influenced by the acid support and being too electrophilic exists predominantly as PdO. If the TiO_2 loading is greater than the optimum, the surface area decreases and the palladium is influenced more by the TiO_2 which could weaken the PdO bond. Similarly, a change in the acidity of the zeolite results in a change in the redox character of the palladium away from this optimum giving a palladium species that is too electrophilic. Significantly the presence of small amounts of metallic Pd(0) were observed in the XPS of the catalysts with TiO_2 despite the facile passivation of the palladium surface by oxide species. This gives a strong indication of the possibility of the presence of PdO and Pd(0) on the surface of the catalyst under reaction conditions.

3.4. Importance of component interaction

The activity of the optimised catalyst depends not only on the presence of individual components on the catalyst surface but also on their interaction with each other. A detailed study into the interaction of all four catalyst components is outside the scope of this work although Cat 7–13 allow a preliminary examination into the importance of this distribution.

As can be seen from Fig. S7 the XRD of 17.5%TiO_2 and Cat 7 are identical. Fig. 7 and Table S3 show that the observed conversions were also the same for the two catalysts. With the TPRs, Fig. S8 also being the same for the two catalysts, it is clear that the order which the components are contacted does not affect the nature or activity. It was assumed that due to the higher surface area of the H-ZSM-5 ($425\ m^2 g^{-1}$) that most of the metals would be preferentially deposited on this surface rather than the lower surface area TiO_2 ($45\ m^2\ g^{-1}$).

Addition of TiO_2 by mechanical mixing (Cat 8) or an additional sonication step (Cat 9) shows identical XRDs to both 17.5%TiO_2 and Cat 7 (Fig. S7). However whilst Fig. 7 and Table S3 shows that the activity of Cat 9 is the same as 17.5%TiO_2 and Cat 7, the activity of Cat 8 is significantly less. The different interactions between the catalyst components are highlighted in the TPR, Fig. S8 where the reduction of the bulk TiO_2 occurs between 220 and 420 °C; however a sharp, intense peak at about 200 °C, which is not present in the profile for 0%TiO_2 is also observed. This has been attributed to the reduction of TiO_2 which is interacting with the metals in a different way. A different interaction is also inferred by the increased temperature of the decomposition of the β-hydride of the palladium metal with the negative peak now at 105 °C compared to about 33 °C for 17.5%TiO_2. The different interactions in Cat 8 results in only a 31 °C decrease in the $T_{50\%}$ value compared to 0%TiO_2 rather than the 51 °C decrease obtained for 17.5%TiO_2, however with such

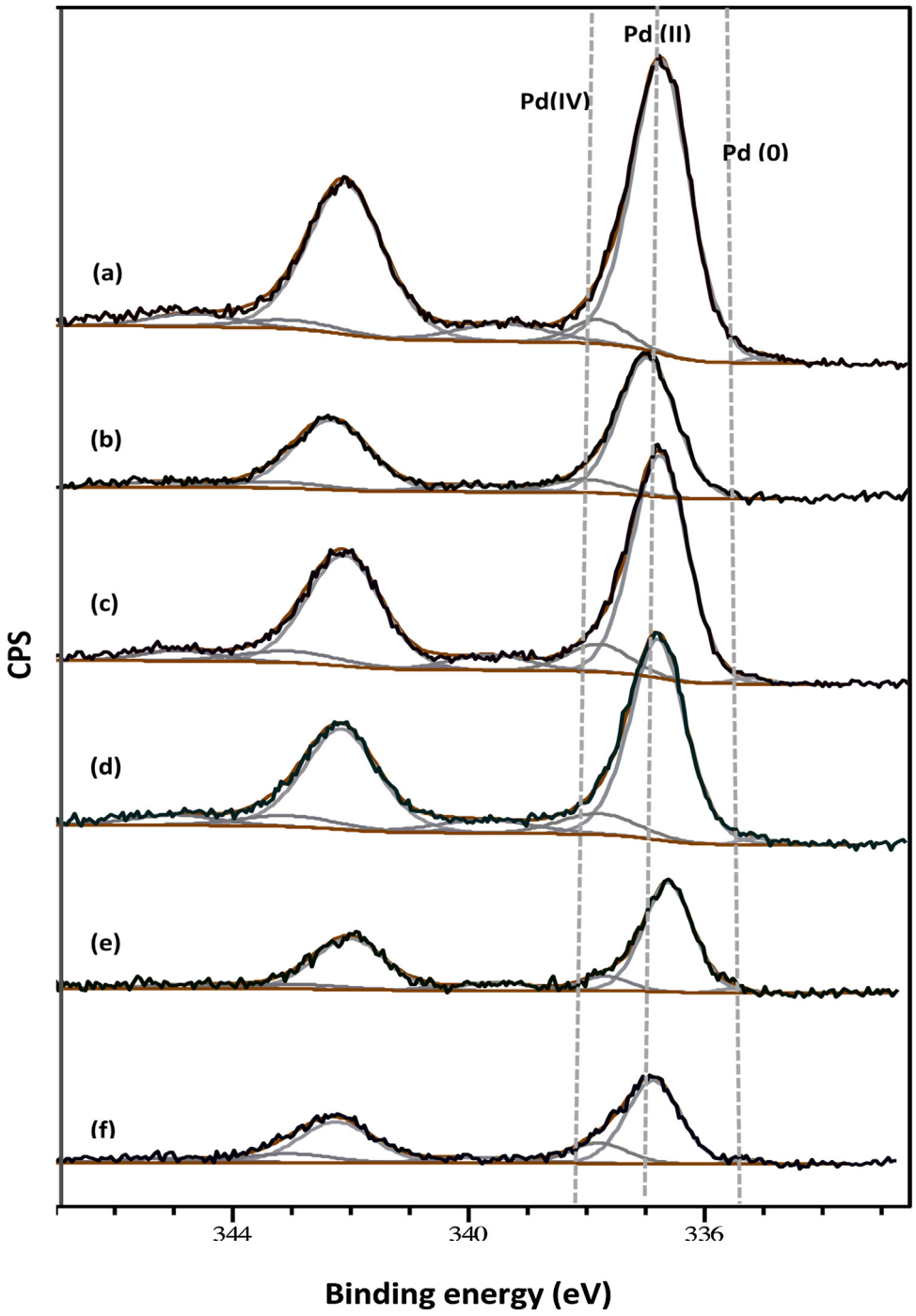

Fig. 6. XPS of the Pd (3d) region with the PdO peaks fitted for (a) Cat 10, (b) 0%TiO_2, (c) 17.5%TiO_2, (d) 83%TiO_2 and (e) 25%TiO_2 and (f) Cat 6. The dashed line indicates the binding energy for Cat 10 7 wt% Pd, H-ZSM-5(80) with 17.5%TiO_2.

an intense PdO reduction peak it is unclear whether the negative peak results from secondary reduction of the PdO.

To further understand the importance of the interaction between components, a catalyst with one fifth the metal loading, Cat 12, was prepared. Fig. 8 and Table S3 show that when the lower loaded catalyst was used there was a significant decrease in activity with the $T_{50\%}$ increasing from 235 °C to 305 °C. However when catalyst 17.5%TiO_2 was diluted such that the metal loading in the bed was the same as that for Cat 12, an increase in activity compared to Cat 12 is observed with the $T_{50\%}$ decreasing to 267 °C showing the decrease in conversion is due to a loss of interaction of the components rather than simply a decrease in metal loading.

3.5. Catalyst stability

Three reactions using different batches of 25% TiO_2 as catalyst showed almost complete reproducibility, Fig. S9 and Fig. 9 shows that no deactivation occurred for either 17.5%TiO_2 or 25%TiO_2 over 50 h time on stream at 250 °C. However, the necessity for the Pt to ensure a stable catalyst was confirmed by a continual deactivation of the monometallic Pd. Here the bimetallic catalyst had a $T_{10\%}$ of 198 °C compared to 206 °C and 265 °C for the monometallic catalysts (Cat 10 and 11), Table S3 and Fig. S10.

The importance of sonication was also observed through comparison with Cat 13, where continual slow deactivation was

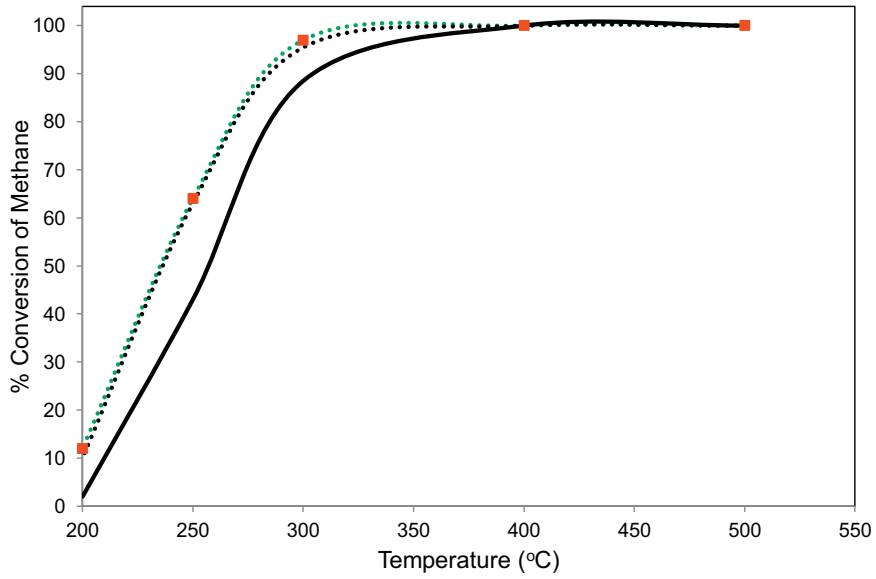

Fig. 7. Comparison of the catalytic activity profiles over catalysts prepared by different methods. The green dashed line shows the data for 17.5%TiO_2, red squares, Cat 7; the black dashed line, Cat 9 and the black solid line Cat 8. (For interpretation of the references to colour in this figure legend, the reader is referred to the web version of this article.)

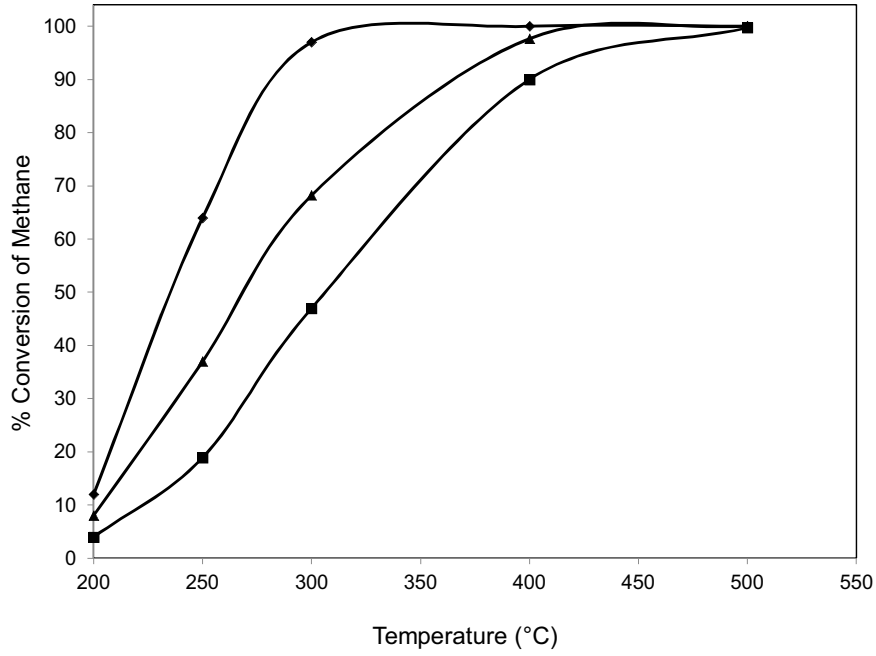

Fig. 8. The effect of metal loading for 17.5%TiO_2 (0.05 g), 5 wt% Pd, 2 wt% Pt, H-ZSM-5(80) with 17.5 wt% TiO_2 (♦) and Cat 12 (0.05 g), 1 wt% Pd, 0.4 wt% Pt, H-ZSM-5 with 18.6 wt% TiO_2 (■). The bed for the diluted catalyst consisted of 17.5%TiO_2 (0.01 g) and H-ZSM-5(80) (0.04 g) (▲).

observed over 50 h, Fig. 9 and a lower activity at each temperature tested, Fig. S11.

Characterisation of the 17.5%TiO_2 catalyst after reaction showed no change in the surface area 301 m^2g^{-1} and the SEM (Fig. S12) and EDX (Fig. S13) showed no significant change in catalyst structure.

4. Conclusions

The acidity of the catalyst support and the presence of an oxygen carrier gives control over the redox behaviour of Pd species on the surface of the catalyst and in so doing controls the activity observed for total methane oxidation. The acidity of the support increases the electrophilicity of the Pd(0) species thereby facilitating its reoxidation while the presence of the TiO_2, oxygen carrier ensures a supply of oxygen as well as improving oxygen mobility for both the oxidation and reduction processes. However, a zeolite support with a greater than optimum number of protons such as ZSM-5(23) results in a palladium species that may be too electrophilic to allow facile reduction resulting in a catalyst with lower activity. By optimising the acidity and oxygen supply a catalyst which shows high activity for the TMO reaction at 200 °C can be obtained, one of the lowest

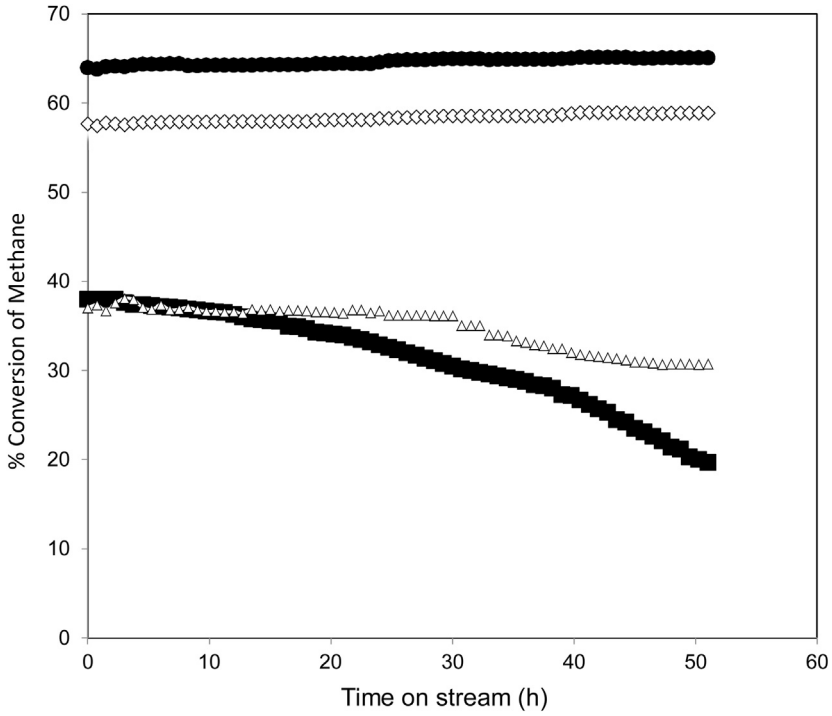

Fig. 9. Comparison of the stability of 17.5%TiO_2, (●), 25%TiO_2 (◊) and 7% Pd catalyst (■) all prepared with sonication and 17.5%TiO_2 prepared without sonication (△).

temperatures reported. The presence of Pt on the catalyst and use of sonication in catalyst preparation was required for a stable catalyst.

Funding sources

The authors would like to acknowledge the support given to AO from South Valley University in Egypt.

Author contributions

The manuscript was written through contributions of all authors. All authors have given approval to the final version of the manuscript.

Appendix A. Supplementary data

Supplementary data associated with this article can be found, in the online version, at http://dx.doi.org/10.1016/j.apcatb.2016.01.017.

References

[1] S.H. Mohr, G.M. Evans, Energy Policy 39 (2011) 5550–5560.
[2] R. Munoz, L. Meier, I. Diaz, D. Jeison, Rev. Environ. Sci. Biotech. 14 (2015) 727–759.
[3] J.H. Lunsford, Catal. Today 63 (2000) 165–174.
[4] M.C. Alvarez-Galvan, N. Mota, M. Ojeda, S. Rojas, R.M. Navarro, J.L.G. Fierro, Catal. Today 171 (2011) 15–23.
[5] E.F. Sousa-Aguiar, F.B. Noronha, J.A. Faro, Catal. Sci. Technol. 1 (2011) 698–713.
[6] E.F. Sousa-Aguiar, L.G. Appel, C. Mota, Catal. Today 101 (2005) 3–7.
[7] M. Gharibi, F.T. Zangeneh, F. Yaripour, S. Sahebdelfar, Appl. Catal. A: Gen. 443–444 (2012) 8–26.
[8] G. Karavalakis, T.D. Durbin, M. Villela, J.W. Miller, J. Nat. Gas Sci. Eng. 4 (2012) 8–16.
[9] J. Le Mer, P. Roger, Eur. J. Soil Biol. 37 (2001) 25–50.
[10] D. Ciuparu, M.R. Lyubovsky, E. Altman, L.D. Pfefferle, A. Datye, Catal. Rev. 44 (2002) 593–649.
[11] P. Galin, M. Primet, Appl. Catal. B: Environ. 39 (2002) 1–37.
[12] W. Lin, Y.X. Zhu, N.Z. Wu, Y.C. Xie, I. Murwani, E. Kemnitz, Appl. Catal. B: Environ. 50 (2004) 59–66.
[13] S.C. Su, J.N. Carstens, A.T. Bell, J. Catal. 176 (1998) 125–135.
[14] K. Persson, A. Ersson, K. Jansson, N. Iverlund, S. Jaras, J. Catal. 231 (2005) 139–150.
[15] R. Abbasi, L. Wu, S.E. Wanke, R.E. Hayes, Chem. Eng. Res. Des. 90 (2012) 1930–1942.
[16] R. Zhou, B. Zhao, B. Yue, Appl. Surf. Sci. 254 (2008) 4701–4707.
[17] Y. Xin, H. Wang, C.K. Law, Combust. Flame 161 (2014) 1048–1054.
[18] O. M'Ramadj, D. Li, X. Wang, B. Zhang, G. Lu, Catal. Commun. 8 (2007) 880–884.
[19] O. M'Ramadj, B. Zhang, D. Li, X. Wang, G. Lu, J. Nat. Gas Chem. 16 (2007) 258–265.
[20] R. Burch, F.J. Urbano, Appl. Catal. A: Gen. 124 (1995) 121–138.
[21] H. Yoshida, T. Nakajima, Y. Yazawa, T. Hattori, Appl. Catal. B: Environ. 71 (2007) 70–79.
[22] S.S. Carstens, J.N. Bell, J. Catal. 176 (1998) 136–142.
[23] R. Harmsen, S. Bates, R.A. van Santen, Faraday Discuss. 106 (1997) 443–450.
[24] L.L. Sheu, H. Knoezinger, W.M.H. Sachtler, J. Am. Chem. Soc. 111 (1989) 8125–8131.
[25] A.Y. Stakheev, W.M.H. Sachtler, J. Chem. Soc. Faraday Trans. 87 (1991) 3703–3708.
[26] J.-g. Wang, C.-j. Liu, Z. Fang, Y. Liu, Z. Han, J. Phys. Chem. B 108 (2004) 1653–1659.
[27] M. Lyubovsky, L. Pfefferle, Catal. Today 47 (1999) 29–44.
[28] M. Cargnello, J.J.D. Jaen, J.C.H. Garrido, K. Bakhmutsky, T. Montini, J.J.C. Gamez, R.J. Gorte, P. Fornasiero, Science 337 (2012) 713–717.
[29] S. Zhang, C. Chen, M. Cargnello, P. Fornasiero, R.J. Gorte, G.W. Graham, X. Pan, Nat. Commun. 6 (2015) 1–6.
[30] A. Janbey, W. Clark, E. Noordally, S. Grimes, S. Tahir, Chemosphere 52 (2003) 1041–1046.
[31] K. Narui, H. Yata, K. Furuta, A. Nishida, Y. Kohtoku, T. Matsuzaki, Appl. Catal. A: Gen. 179 (1999) 165–173.
[32] K. Persson, S. Jaras, J. Catal. 245 (2007) 401–414.
[33] M. Monai, T. Montini, M. Melchionna, P. Duchoň Kúš, K.C. Prince, V. Matolin, R.J. Gorte, P. Fornasiero, Appl. Catal. B: Environ. (2015) (http://dx.doi.org/10.1016/j.apcatb.2015.10.001).
[34] M. Monai, T. Montini, C. Chen, E. Fonda, R.J. Gorte, P. Fornasiero, ChemCatChem 7 (2015) 2038–2046.
[35] C. Chen, Y.-H. Yeh, M. Cargnello, C.B. Murray, P. Fornasiero, R.J. Gorte, ACS Catal. 4 (2014) 3902–3909.
[36] A.T. Gremminger, H.W. Pereira de Carvalho, R. Popescu, J.-D. Grunwaldt, O. Deutschmann, Catal. Today 258 (Part 2) (2015) 470–480.
[37] A.I. Osman, J.K. Abu-Dahrieh, D.W. Rooney, S.A. Halawy, M.A. Mohamed, A. Abdelkader, Appl. Catal. B: Environ. 127 (2012) 307–315.
[38] K. Persson, A. Ersson, S. Colussi, A. Trovarelli, S.G. Jaras, Appl. Catal. B: Environ. 66 (2006) 175–185.
[39] Y.-S. Bi, G.-Y. Dang, X.-H. Zhao, X.-F. Meng, H.-J. Lu, J.-T. Jin, J. Hazard. Mater. 229–230 (2012) 245–250.
[40] J.A. Wang, A. Cuan, J. Salmones, N. Nava, S. Castillo, M. Morán-Pineda, F. Rojas, Appl. Surf. Sci. 230 (2004) 94–105.

[41] D. Simone, N.L. Brungard, R. Farrauto, T. Kenelly, Appl. Catal. 70 (1991) 87–100.
[42] D. Roth, P. Gelin, M. Primet, E. Tena, Appl. Catal. A: Gen. 203 (2000) 37–45.
[43] J.H. Lee, D.L. Trimm, Fuel Process. Technol. 42 (1995) 339–359.
[44] C.A. Gonzalez, A.N. Ardila, C. Montes de Correa, M.A. Martinez, G. Fuentes-Zurita, Ind. Eng. Chem. Res. 46 (2007) 7961–7969.
[45] B. Wen, J. Jia, W.M.H. Sachtler, J. Phys. Chem. B 106 (2002) 7520–7523.
[46] C.-B. Wang, C.-M. Ho, H.-K. Lin, H.-C. Chiu, Fuel 81 (2002) 1883–1887.
[47] C. He, J. Li, X. Zhang, L. Yin, J. Chen, S. Gao, Chem. Eng. J. 180 (2012) 46–56.
[48] P. Sangeetha, K. Shanthi, K.S.R. Rao, B. Viswanathan, P. Selvam, Appl. Cata. A: Gen. 353 (2009) 160–165.
[49] L. Yue, C. He, X. Zhang, P. Li, Z. Wang, H. Wang, Z. Hao, J. Hazard. Mater. 244–245 (2013) 613–620.
[50] L.S. Kibis, A.I. Stadnichenko, S.V. Koscheev, V.I. Zaikovskii, A.I. Boronin, J. Phys. Chem. C 116 (2012) 19342–19348.